NJC

ROYAL SOCIETY OF CHEMISTRY

PAPER

View Article Online
View Journal | View Issue

Cite this: *New J. Chem.*, 2024, **48**, 13030

Trans influence of cyanide on the structural and electronic properties of a series of organocobalt^{III}(TIM) complexes†

Leobardo Rodriguez Segura and Tong Ren *

The *trans* influence of anionic ligands on the nature of the cobalt–carbon bond in *trans*-[Co(TIM)RX]$^+$-type complexes (R is a C-bound ligand and TIM is 2,3,9,10-tetramethyl-1,4,8,11-tetraazacyclotetradeca-1,3,8,10-tetraene) was probed through the incorporation of cyanide as the second monoanionic axial ligand (X). Salt metathesis reactions between KCN and the corresponding halide precursors readily generate *trans*-[Co(TIM)(C(CH$_2$)Ph)(CN)]$^+$ (**1**), *trans*-[Co(TIM″)(C(CH$_3$)C$_6$H$_4$-4-^{t}Bu)(CN)]$^+$ (**2**, TIM″ is the reduced TIM derivative following the formation of an aza-cobalt-cyclopropane moiety), and *trans*-[Co(TIM)(CH$_3$)(CN)]$^+$ (**3**). The molecular structures of **1** and **2** were established *via* single-crystal X-ray diffraction studies. FT-IR spectroscopy revealed a red-shift in the ν(C≡N) stretching frequency from **1** to **3** to **2**. The absorption spectra of **1**–**3** exhibit d–d bands which are substantially blue-shifted from their halide precursors as a result of the enhanced ligand field imbued by the cyanide. Cyclic voltammograms of **1** and **3** consist of an irreversible Co$^{4+/3+}$ oxidation and an irreversible Co$^{3+/2+}$ reduction. In **2**, a reversible Co-centered reduction is observed at −1.75 V *vs.* Fc$^{1+/0}$. Also reported are the crystal structures of *trans*-[Co(TIM)(CN)$_2$]PF$_6$ (**4**), *trans*-[Co(TIM)(CH$_3$)I]PF$_6$ (**5**) and *trans*-[Co(TIM)(CH$_3$)$_2$]PF$_6$ (**6**). The π-accepting capabilities of the cyanide reduce the dπ(Co)-π*(imine) backdonation in **4**, while the solely strong σ-donating nature of the −CH$_3$ ligands in **6** exerts a large *trans* influence and significantly increases the Co-TIM interactions.

Received 21st May 2024,
Accepted 26th June 2024

DOI: 10.1039/d4nj02364a

rsc.li/njc

Introduction

The inorganic and organometallic properties of vitamin B$_{12}$ (predominately as the active cofactors, methylcobalamin and adenosylcobalamin) and its model complexes have inspired chemists since the structural determination of vitamin B$_{12}$ by Hodgkin.[1,2] More recently, there has been increased emphasis on the role of these organocobalt(III) complexes as nature-inspired, environmentally benign catalysts for organic transformations. Specifically, the ability of the cobalt–carbon bond to undergo homolytic cleavage under mild conditions to afford carbon-centered radicals enables access to a vast number of desirable carbon–carbon bond forming reactions, such as radical additions, ring expansion, and C–H activation.[3,4] Creative applications of vitamin B$_{12}$ in cooperative photocatalytic systems have achieved even more diverse reactivities, including regioselective epoxide arylation and reduction.[5]

Among the vitamin B$_{12}$ model complexes, extensive attention has been given to bis-dimethylglyoxime cobalt complexes, or *cobaloximes* (Type A, Scheme 1).[6–8] Notably, the two equatorial glyoximato ligands yield a pseudomacrocyclic framework around the cobalt center with a combined dianionic charge. In contrast, cobalamins are supported by a highly conjugated, monoanionic corrin ring (Type B, Scheme 1). Nonetheless, both species typically bear a L-type ligand (L = neutral ligand; commonly a weak Lewis base) in the *trans* position relative to the R group, and substantial work on the influence of these

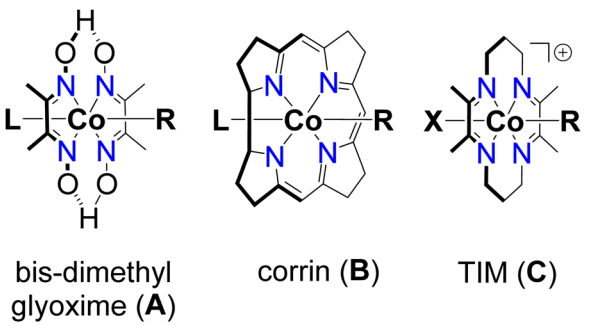

Scheme 1 Equatorial ligands in vitamin B$_{12}$ and model systems.

Department of Chemistry, Purdue University, West Lafayette, Indiana 47907, USA. E-mail: tren@purdue.edu

† Electronic supplementary information (ESI) available. CCDC 2355970–2355974. For ESI and crystallographic data in CIF or other electronic format see DOI: https://doi.org/10.1039/d4nj02364a

ligands on the nature of the cobalt–carbon bond, and *vice versa*, has been performed.[9,10]

On the other hand, significantly less attention has been devoted to vitamin B_{12} model systems bearing X-type ligands (X = monoanionic ligand) in the analogous *trans* position.[11,12] A related family of Co^{III} complexes is based on TIM (2,3,9,10-tetramethyl-1,4,8,11-tetraazacyclotetradeca-1,3,8,10-tetraene; type C in Scheme 1), where the Co^{III} center is substantially more electron-deficient than those in types **A** and **B** due to TIM being neutral. The combined effects of an electron-deficient Co^{III} center and a *trans* anionic ligand are expected to impact the cobalt–carbon bond in organocobalt^{III}(TIM) complexes. Plausibly, these *cis* and *trans* influences have played a role in the surprisingly limited number of examples of previously reported alkyl *trans*-[RCo^{III}(TIM)X]$^+$-type complexes (R = $-CH_3$ or $-CH_2C_6H_5$; X = halide or $-CH_3$).[13,14]

As part of ongoing efforts in developing organometallic compounds based on the combination of 3d metal ions and tetraaza macrocycles,[15,16] we recently detailed the formation of *trans*-[Co^{III}(TIM)(C(CH_2)Ar)Cl]PF_6 complexes (Ar = $-C_6H_5$, $-C_6F_5$, and $-C_6H_4$-4-^{t}Bu), in which the organic group bonded to the cobalt center is sp^2-hybridized (see Scheme 2), as alternatives to the less-accessible alkyl complexes.[17] Interestingly, *trans*-[Co(TIM″)-(C(CH_3)Ar)Cl]$^+$-type complexes (Ar = $-C_6H_5$ and $-C_6H_4$-4-^{t}Bu) were also observed wherein an aza–cobalt–cyclopropane moiety was generated from the formation of a new C–N bond between the axially bonded alkenyl and the TIM macrocycle. As a result, the adjacent imine unit in the TIM ligand was reduced to an amine to give the TIM″ derivative and a Co–C(sp^3) bond. To gain further insight into the *trans*-influence of anionic ligands (X-type), as opposed to neutral ligands (L-type), on the cobalt–carbon bond with various R groups, we have substituted the halide in *trans*-[Co(TIM)(C(CH_2)Ph)X]$^+$, *trans*-[Co(TIM″)(C(CH_3)C_6H_4-4-^{t}Bu)X]$^+$, and *trans*-[Co(TIM)(CH_3)X]$^+$ complexes with cyanide to yield *trans*-[Co(TIM)(C(CH_2)Ph)(CN)]$^+$ (**1**), *trans*-[Co(TIM″)(C(CH_3)C_6H_4-4-^{t}Bu)-(CN)]$^+$ (**2**), and *trans*-[Co(TIM)(CH_3)(CN)]$^+$ (**3**), respectively. Moreover, the stretching frequency of the cyanide is expected to be impacted by the R ligand; therefore, information on the *trans* influence of R may be extrapolated.[18] Similar studies for Co^{II} macrocyclic complexes by Endicott and coworkers revealed that synergistic *trans* influences for the low spin Co^{II} species (generated *in situ via* pulse radiolysis) could play a major role in inner-sphere electron transfer reactions.[19] These cyanide complexes may offer innovative opportunities given that cyanide-bearing vitamin B_{12} derivates have been shown to behave as homogeneous electrocatalysts for water oxidation[20] and as photothermal conversion catalysts to promote atom transfer radical polymerization.[21] The new cyanide complexes, **1**–**3** (see Scheme 2), have been characterized using single-crystal X-ray diffraction studies, absorption and FT-IR spectroscopies, and through electrochemical studies. Additionally, we report the first crystallographic structures of *trans*-[Co(TIM)($CN)_2$]PF_6 (**4**),[22] *trans*-[Co(TIM)(CH_3)I]PF_6 (**5**),[13] and *trans*-[Co(TIM)($CH_3)_2$]PF_6 (**6**)[14] in order to probe and classify the structural properties of these complexes.

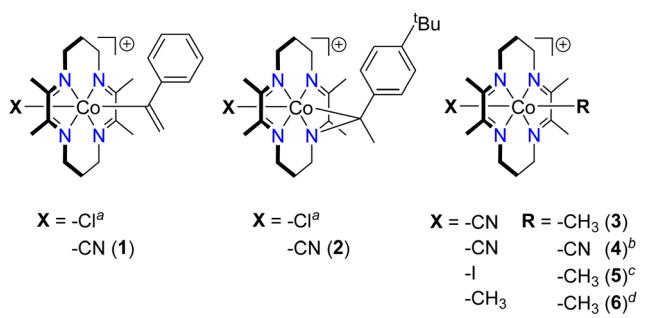

Scheme 2 Organocobalt^{III}(TIM) complexes; complexes previously reported in references 17[a], 22[b], 13[c], and 14[d].

Results and discussion

Synthesis

The reaction between *trans*-[Co(TIM)(C(CH_2)Ph)Cl]PF_6 and 2 equiv. of KCN in a 2/1 CH_3OH/CH_3CN solvent mixture resulted in the very rapid formation of *trans*-[Co(TIM)(C(CH_2)Ph)(CN)]PF_6 (**1**) as a yellow solution. The use of excess KCN (>3 molar equivalents) resulted in facile degradation, yielding a light brown solution. A similar brown degradation product was observed when the reaction was left to stir for greater than 0.5 h. Therefore, the solvent was removed from the crude reaction mixture of **1** (<10 min after the addition of KCN), and the remaining red-orange residue was redissolved in acetone prior to filtering over Celite to remove the excess K^+ salts. Analytically, pure **1** was obtained by ether/acetone recrystallization. Comparable reactions and observations were made for the synthesis and purification of *trans*-[Co(TIM″)(C(CH_3)C_6H_4-4-^{t}Bu)(CN)]PF_6 (**2**), *trans*-[Co(TIM)(CH_3)(CN)]PF_6 (**3**), and *trans*-[Co(TIM)($CN)_2$]PF_6 (**4**), which were isolated in moderate to high yields ranging between 74 and 88%. A previously published synthetic procedure for **4** involves reacting aqueous [Co(TIM)Cl_2]PF_6 with NaCN in large excess, followed by purification on an ion exchange column.[22] All the cyanide complexes appear to be indefinitely stable as solids but degrade significantly in CH_3OH and CH_3CN solutions at room temperature. Solutions stored at −15 °C are stable for up to several weeks. Notably, solutions of complex **2**, bearing the aza–cobalt–cyclopropane moiety, appear to be the most stable, while those of the di-cyano complex **4** are the least stable.

The previously reported synthesis of *trans*-[Co(TIM)(CH_3)Cl]$^+$ starts with the addition of $NaBH_4$ to *trans*-[Co(TIM)Cl_2]$^+$ to generate a nucleophilic Co^I(TIM) intermediate, which reacts with MeI under an inert atmosphere.[13] Efforts to obtain the mono-alkyl complex in a similar fashion resulted in an abundance of *trans*-[Co(TIM)(CH_3)I]PF_6 (**5**) in our hands, where the use of excess MeI favored a replacement of the *trans* chloride ligand with an iodide. Moreover, it was found that careful purification over silica using a 1/9 acetone/CH_2Cl_2 solvent mixture afforded **5** in 27% yield, while isolation of a chloro derivative was not achieved. In the literature, the subsequent reaction of *trans*-[Co(TIM)(CH_3)X]$^+$ with MeI upon reduction with $NaBH_4$ resulted in *trans*-[Co(TIM)($CH_3)_2$]$^+$ (**6**).[14] Interestingly, an alternative literature procedure describes the synthesis of **6**

directly from $[Co(TIM)Cl_2]^+$ using $NaBH_4$ and MeI with no mention of a protective inert atmosphere.[23] The latter procedure for **6** was employed in this work, except that the PF_6^- counterion was used instead of the reported ClO_4^- salt.

Molecular structures

The structures of both new compounds **1** and **2**, and previously synthesized but structurally unknown compounds **4**–**6** were determined *via* single-crystal X-ray diffraction and are shown in Fig. 1 and 2. Selected bond lengths and angles are provided in Table 1, and additional details regarding data collection and structure refinement are provided in the ESI† (Table S1). All complexes assume a pseudo-octahedral geometry with the TIM (or TIM″ in **2**) ligand occupying the equatorial positions.

In the alkenyl-bearing cyanide complex, **1**, a Co–C bond length to the alkenyl ligand of 2.036(2) Å is observed, which is slightly contracted from that (2.044(2) Å) in the precursor complex, $[Co(TIM)(C(CH_2)Ph)Cl]^+$.[17] Given that cyanide is a strong σ-donor and chloride is only a weak π-donor, the Co–C bond contraction was unanticipated. It is plausible that the strong π-acidity of cyanide reduces the electron density at the

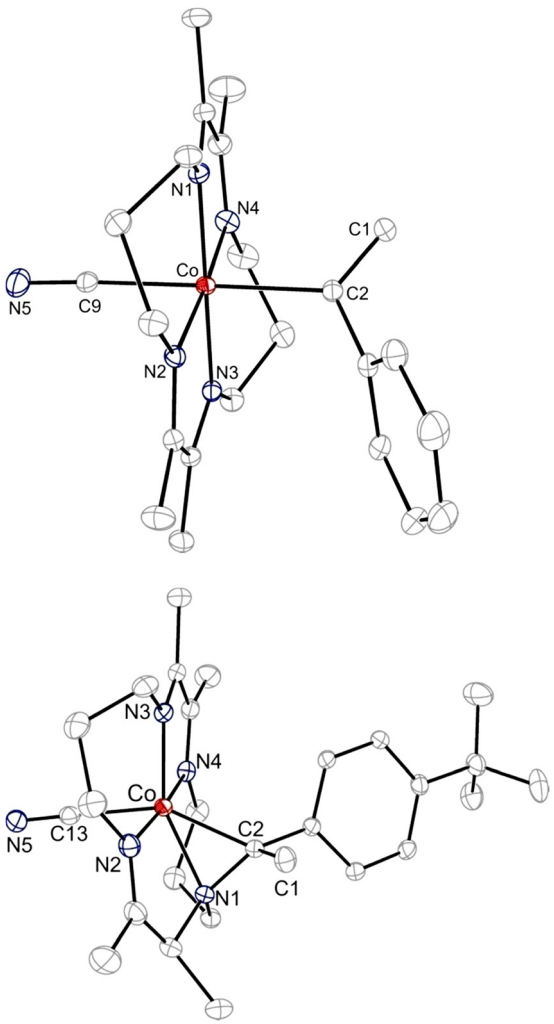

Fig. 1 ORTEP plot of **1** (top) and **2** (bottom) at the 30% probability level. The H atoms, PF_6^- counterions, and solvent molecules are omitted for clarity.

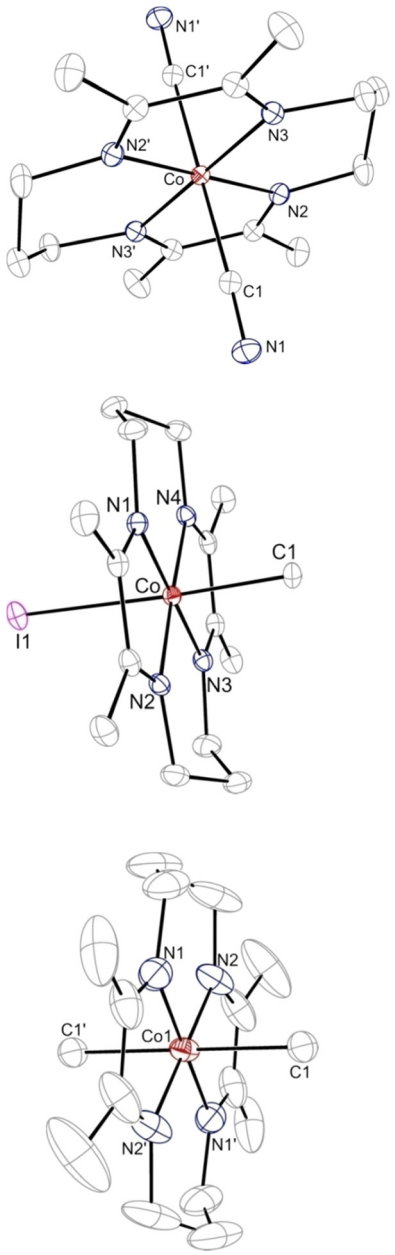

Fig. 2 ORTEP plot of **4** (top), **5** (middle), and **6** (bottom) at the 30% probability level. The H atoms, atom disorder, and PF_6^- counterions are omitted for clarity.

Table 1 Selected bond lengths (Å) and angles (°) for compounds **1**, **2**, and **4**–**6**

	1	**2**	**4**	**5**	**6**
Co–C	2.036(2)	1.995(2)	—	2.009(3)	2.077(3)
Co–I/C(≡N)	1.951(2)	1.982(2)	1.915(1)	2.7090(5)	—
$Co–N_{av}$	1.914[3]	—	1.925[2]	1.916[3]	1.889[4]
C≡N	1.144(2)	1.129(3)	1.150(2)	—	—
$C{=}N_{TIM,av}$	1.291[4]	1.287[4][a]	1.290[3]	1.293[4]	1.293[7]
$C–C_{TIM,av}$	1.479[3]	1.471(3)[a]	1.481(2)	1.476[5]	1.442[6]

[a] Bond lengths reported for the intact α-diimine unit.

Co center, resulting in a slight shortening of the cobalt–alkenyl bond. Across the cobalt center, the mutual *trans* influence of the alkenyl can be seen in the Co–C(≡N) bond length of 1.951(2) Å.

The molecular structure of **2** confirms that the aza–cobalt–cyclopropane moiety is preserved upon substitution of chloride with cyanide. Within the three-member ring, no significant structural differences in the bonds and angles are noted between **2** and the chloride precursor.[17] The TIM″ macrocycle, in which an imine unit is reduced to generate a new bond between the amido nitrogen and the α-carbon of the axial ethylbenzene ligand, is also not impacted structurally by cyanide. On the other hand, the Co–C(≡N) bond length is 1.982(2) Å, which is longer than that in **1**. This is consistent with the stronger *trans* influence exerted by the alkyl group of the three-membered ring. Interestingly, cyanide in **2** leads to a cobalt–carbon bond distance of 1.995(2) Å, which is significantly lengthened compared to the analogous bond in $[Co(TIM'')(C(CH_3)C_6H_4\text{-}4\text{-}^tBu)Cl]^+$ (1.967(2) Å).[17] The lengthening of the Co–C bond is in agreement with the stronger electron-donating ability of the cyanide relative to chloride. The altered TIM″ ligand may exert a *cis* influence, which results in the elongation of the cobalt–carbon bond, unlike the contraction observed above in **1**.

The previously unknown molecular structure of the di-cyano complex, **4** (see Fig. 2), is determined and provides further insight into the structural influence of the cyanide ligand. Relative to the alkenyl-bearing complex, **1**, the Co–C(≡N) bond in **4** is noticeably shortened to 1.915(1) Å. The highly symmetrical cyanide ligands are both π-acceptors, which allows the axial ligands to withdraw the electron density away from the metal center. Consequently, a slight increase in $Co\text{–}N_{av}$ is observed in **4**, implying that the dπ(Co)-π*(imine) backdonation is reduced. Interestingly, the average Co–C(≡N) bond length is nearly the same as that in other structurally similar complexes, namely *trans*-bis(dimethylglyoximato)(dicyano)cobalt(III)[24] (∼1.914 Å) and 2,3,9,10-tetramethyl-1,4,8,11-tetraazaundecane-1,3,8,10-tetraen-11-ol-1-olatodicyanocobalt(III)[25] (∼1.913 Å). This correlation would suggest that the anionic charges, or lack thereof, on the equatorial ligand(s) do not have a considerable impact on the axially bonded cyanide ligands.

The structures of **5** and **6** (Fig. 2, middle and bottom, respectively) represent the first examples of Co(TIM) complexes bearing axial alkyl ligands. In particular, the structure of **6** is a rare example of a cobalt di-alkyl supported by a macrocyclic ligand.[26,27] In the structure of **5**, the bond lengths within the macrocycle are in good agreement with the structure of the precursor compound, $[Co(TIM)Cl_2]^+$, although a small decrease in the $Co\text{–}N_{av}$ bond length in **5** is observed from 1.926[3] ($[Co(TIM)Cl_2]^+$) to 1.916[3] Å (**5**).[28] This decrease is much more significant for the di-methyl complex, **6**, which has a $Co\text{–}N_{av}$ bond length of 1.889[4] Å. The shortening of the bond between the metal center and the TIM nitrogen atoms is likely caused by an increase in the electron density at the Co center, which in turn enhances the dπ(Co)-π*(imine) backdonation. Interestingly, the imine bonds ($C{=}N_{TIM,av}$) do not seem to be influenced by the nature of the axial ligands, but a shortening from $[Co(TIM)Cl_2]^+$ (1.486[3] Å) to **6** (1.442[6] Å) in the C–C bonds of the α-diimine units is noted. The average of the same C–C bonds in **5** was found to be 1.476[5] Å. These values reveal a considerable amount of π-electron delocalization within the TIM ligand in **6**, which has been postulated to aid in stabilizing the di-methyl Co^{III}(TIM) complex.[26]

The $Co\text{–}CH_3$ bond length of 2.009(3) Å in **5** is slightly elongated relative to the Co–Me bond in methylcobalamin (1.979(4)–1.987(1) Å).[29,30] However, it is, within experimental errors, the same as the corresponding bond in other vitamin B_{12} model complexes, such as *trans*-bis(glyoximato)(methyl)(pyridine)cobalt(III)[31] (2.005(4) Å) and *trans*-bis(dimethylglyoximato)-(methyl)(pyridine)cobalt(III)[32] (1.998(5) Å). The lack of a pronounced *trans* influence by the anionic iodide is in agreement with previous reports on structurally related methyl-bearing Co(III) macrocyclic complexes, which reveal that the Co–C bond length is more sensitive to steric *cis* influences from the equatorial ligand than the electronic nature of the *trans* ligand.[33,34] Alternatively, the *trans* influence of iodide serves to counterbalance the weaker *cis* influence from the neutral TIM ligand. The coordination of a second methyl group results in a Co–C bond distance of 2.077(3) Å, which is considerably elongated compared to that in **5** but consistent with the same bond in 2,3,9,10-tetramethyl-1,4,8,11-tetraazaundecane-1,3,8,10-tetraen-11-ol-1-olatodimethylcobalt(III) (2.049[8] Å).[26]

C≡N stretching characteristics

The ν(C≡N) stretching frequencies for **1**–**3** were examined using FT-IR spectroscopy, and the resulting spectra are shown in Fig. 3 (for the full spectra, see Fig. S1, ESI†). Increasing the donor strength of the ligand *trans* to the cyanide results in a slight red-shift in ν(C≡N). The shift to lower frequencies is expected based on the increased electron density at the Co center, which enables greater π-backbonding into the cyanide antibonding orbitals and weakens the C≡N bond.[35] Thus, ν(C≡N) are 2135, 2133, 2129, and 2123 cm^{-1} when the *trans* ligands are –CN, $-C_2Ph$,[36] $-C(CH_2)Ph$, and $-CH_3$, respectively. The stretching frequency of **2** (2113 cm^{-1}) is further red-shifted, suggesting that there is an even greater electron density

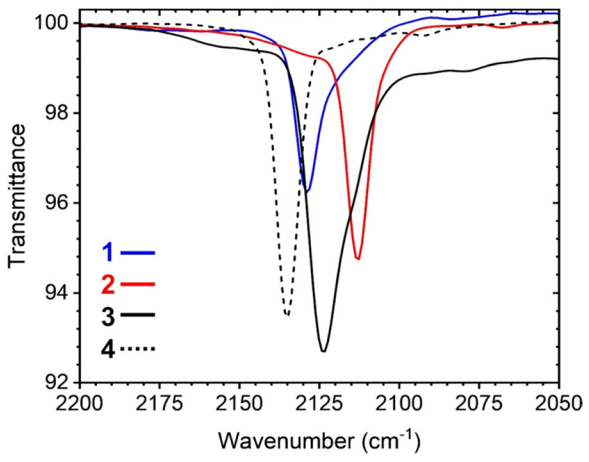

Fig. 3 ATR-FTIR spectra of **1**–**4** showing C≡N stretches.

donated through the Co^{III} center by the aza–cobalt–cyclopropane moiety. This is consistent with an increase in the Co–C(≡N) bond length from **1** to **2**, as discussed above.

In other vitamin B_{12} model complexes, considerable attention has been given to the *cis* influence of the macrocycle.[37,38] A comparison of the stretching frequencies between **3** (2123 cm^{-1}) and methylcyanocobanimide[38] (2088 cm^{-1}) reveals a substantial difference of 35 cm^{-1}. This is consistent with the fact that TIM is significantly less donating than corrin, which renders a much weaker dπ(Co)-π*(C≡N) backdonation in **3** than that in methylcyanocobanimide. A similar comparison, albeit to a lesser degree, can be made between the ν(C≡N) in the dicyano complex, **4** (2135 cm^{-1}) and that reported for another vitamin B_{12} model complex, 8,12-diethyl-1,2,3,7,13,17,18,19-octamethyltetradehydrocorrincobalt(III) dicyanide (2120 cm^{-1}).[39]

The ν(C=N) stretch of the imine units of the TIM macrocycle was also analyzed. In the original report on $[Co(TIM)Cl_2]PF_6$, the authors assigned a weak band at 1597 cm^{-1} as the ν(C=N) symmetric stretch of the imine units of the TIM macrocycle.[40] Additionally, a weaker band at 1650 cm^{-1} was assigned to the ν(C=N) asymmetric stretch. Analysis of the spectra for **1–6** within this region reveals weak bands that may be tentatively assigned as the corresponding stretching modes (see Fig. S1, ESI†); however, the significant broadening of the bands in **1** and **3** and the absence of a band in **5** make it difficult to extrapolate experimentally meaningful information from these vibrations.

Electronic absorption spectra

The absorption spectra of compounds **1–3** were collected at room temperature in CH_3CN under ambient conditions, and the resulting spectra are shown in Fig. 4, along with those of the precursor of **1**, $[Co(TIM)(C(CH_2)Ph)Cl]PF_6$. Alkenyl-bearing complex **1** displays a well-defined transition at 365 nm (ε ∼ 3500), which is likely due to the peak at 477 nm (ε ∼ 1300) for $[Co(TIM)(C(CH_2)Ph)Cl]PF_6$. While both peaks are significantly more intense than the lowest energy d–d bands in $[Co(CN)_6]^{3-}$ (λ = 312 nm; ε ∼ 140),[41] and $[Co(TIM)Cl_2]^+$ (λ = 575 nm; ε ∼ 50),[40] they are still primarily d–d transitions with substantial charge-transfer characteristics related to the alkenyl ligand. The considerable blue shift of the peak of **1** compared to that of $[Co(TIM)(C(CH_2)Ph)Cl]PF_6$ is clearly attributed to ligand field enhancement *via* the substitution of Cl^- by CN^-. The corresponding d–d band in **2** appears at 420 nm (ε ∼ 2500), and the red-shift from that of **1** is attributed to the reduced π-acidity of TIM″ compared to that of TIM, which results in a weaker ligand field in **2**. Similar to **1**, the d–d band in **2** is blue-shifted from that of the precursor $[Co(TIM'')(C(CH_3)C_6H_4\text{-}4\text{-}^tBu)Cl]PF_6$ (spectra shown in Fig. S2A, ESI†), reflecting ligand field enhancement by CN^- ligation. The same blue shift of the d–d band due to CN^- ligation is clear from a comparison of the spectra of **3** and **5** (Fig. S2B, ESI†).

Electrochemical studies

Compounds **1–3** were studied electrochemically, and cyclic voltammograms for the reduction events are shown in Fig. 5 (see Fig. S4–S6 for oxidation events, ESI†). For comparison, voltammetric studies of **4** and **5** were also performed (see Fig. 6 and Fig. S7, S8, ESI†). The electrode potentials (*vs.* $Fc^{1+/0}$) are listed in Table 2.

At negative potentials, compound **1** undergoes one irreversible 1 e^- reduction at −1.52 V, which is best assigned as $Co^{3+/2+}$ reduction. This event is cathodically shifted when compared to the same reduction event in the precursor, $[Co(TIM)(C(CH_2)Ph)Cl]^+$ (−1.01 V).[17] The 500 mV shift in the potential is attributed to the stronger donating nature and *trans* influence of cyanide compared to chloride. Likewise, compound **2** exhibits one reduction at −1.75 V, which is cathodically shifted from that of $[Co(TIM'')(C(CH_3)C_6H_4\text{-}4\text{-}^tBu)Cl]^+$ (−1.43 V).[17] Interestingly, the precursor of **2** exhibited second reduction event at −1.57 V, which was tentatively assigned to TIM″-based reduction. In **2**, the high sensitivity of the reduction potential to the nature of the axial ligand (*i.e.* chloride to cyanide) suggests that the one-electron event is best assigned to be cobalt-centered. Based on previous calculations on the chloride-bearing species, $[Co(TIM'')(C(CH_3)Ph)Cl]PF_6$, a high degree of orbital mixing occurs between the five 3d orbitals and the axial and equatorial ligands.[17] Therefore, the strong donating capabilities of cyanide increase the electron

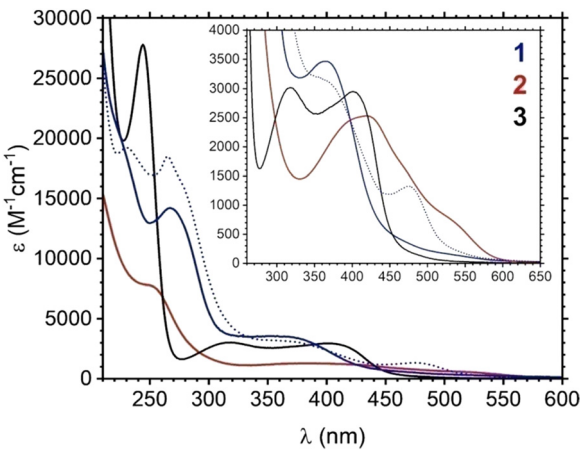

Fig. 4 Absorption spectra of **1–3** and $[Co(TIM)(C(CH_2)Ph)Cl]PF_6$ (dotted trace) in CH_3CN.

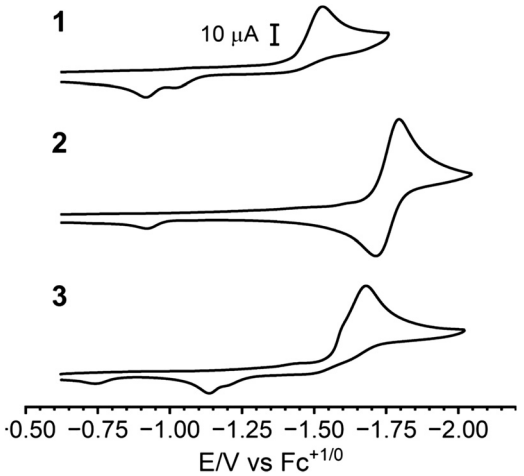

Fig. 5 Cyclic voltammograms of compounds **1–3** (1.0 mM) recorded in 0.10 M CH_3CN solutions of $[^nBu_4N][PF_6]$ at a scan rate of 0.1 V s^{-1}.

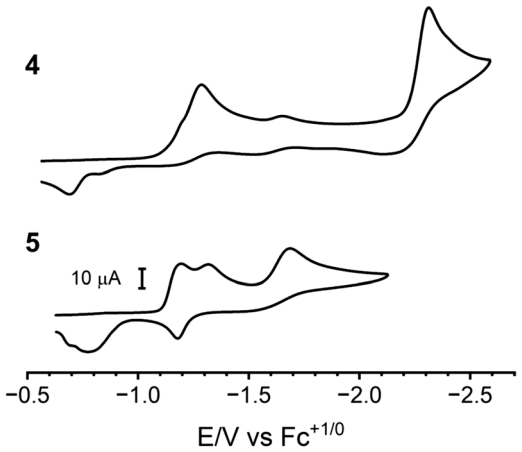

Fig. 6 Cyclic voltammograms of compounds **4** and **5** (1.0 mM) recorded in 0.10 M CH_3CN solutions of $[^nBu_4N][PF_6]$ at a scan rate of 0.1 V s^{-1}.

Table 2 Electrode potentials of Co-centered redox couples (V, *vs.* $Fc^{1+/0}$) in **1–5**, **[Co(TIM)(C(CH$_2$)Ph)Cl]$^+$**, and **[Co(TIM″)(C(CH$_3$)C$_6$H$_4$-^{t}Bu)Cl]$^+$**[a]

	$E_{pa}(Co^{4+/3+})$	$E_{pc}(Co^{3+/2+})$
1	1.33	−1.52
[Co(TIM)(C(CH$_2$)Ph)Cl]$^+$[b]	1.32	−1.01(0.17)[c]
2	0.82	−1.75(0.08)[d]
[Co(TIM″)(C(CH$_3$)C$_6$H$_4$-^{t}Bu)Cl]$^+$[b]	1.12	−1.43(0.15)[d]
3	−0.02	−1.68
4	0.67	−1.29
5	−0.06	−1.20

[a] Solutions contain 1.0 mM analyte and 0.1 M *n*-Bu_4NPF_6 as the supporting electrolyte in CH_3CN. [b] Ref. 17. [c] Quasi-reversible couple. [d] $E_{1/2}(Co^{3+/2+})$ are also reported. Peak separation (ΔE_p) is shown in parentheses.

density around the cobalt center to the degree that TIM″-based reduction is shifted to much higher potentials in **2**.

The cathodic process in the methyl-bearing cyanide complex, **3**, is less well-defined, with a shoulder visible around −1.59 V and an irreversible $Co^{3+/2+}$ reduction at −1.68 V (Fig. 5). In the di-cyano complex, **4**, the cobalt-centered reduction becomes less cathodic at −1.29 V, which is attributed to a decrease of the electron density at the metal center due to the π-accepting nature of the cyanides. The irreversibility of this couple is strongly indicative of the fast dissociation of CN^- upon reduction at the Co center, which may also be the cause of the irreversibility of the $Co^{3+/2+}$ couple in **1** and **3**. The σ-donating nature of cyanide is greater than that of iodide, as evidenced by the more anodically shifted $Co^{3+/2+}$ reduction potential in **5** (−1.20 V).

Complexes **4** and **5** exhibit reduction events at more negative potentials, while **1**–**3** do not. It is plausible that a combination of strong σ-donating R groups and the strong σ-donating cyanide in **1**–**3** shifted the reduction beyond $Co^{3+/2+}$ out of the solvent window. Meanwhile, for **5** (see Fig. 6), an irreversible reduction at −1.32 V closely follows the $Co^{3+/2+}$ event. The second event is tentatively assigned to a $Co^{2+/1+}$ reduction based on the readily accessible Co^{I}(TIM)(CH_3) species isolated by Farmery and Busch.[14] At further negative potentials, a third event occurs at −1.69 V. Owing to the redox non-innocent nature of the TIM ligand, it is possible that this event is a $TIM^{0/1-}$ reduction.[42,43] During the return wave, an anodic process was seen at −1.18 V, but increasing the scan rate to 0.5 V s^{-1} did not improve the electrochemical reversibility of the event (see Fig. S9, ESI†).

Although the *trans* cyanide significantly impacts the reduction events in the Co(TIM) complexes, it exerts less influence on the oxidation processes. The irreversible 1 e^- oxidation ($Co^{4+/3+}$) observed for **1** at 1.33 V (Fig. S4, ESI†) is nearly identical in potential to the same event in the chloro-bearing precursor (1.32 V).[17] Likewise, the $Co^{4+/3+}$ oxidation potential in the methyl-bearing cyanide species, **3**, is only slightly shifted at −0.02 V (Fig. S6, ESI†) compared to the respective oxidation event in **5** (−0.06 V). Instead, the 1.30 V cathodic shift in the oxidation potential from **1** to **3** is primarily attributed to the stronger σ-donating nature of the axial methyl ligand in the latter. For the aza–cobalt–cyclopropane-bearing TIM″ complex, **2**, the substitution of chloride with cyanide results in a 300 mV cathodic shift in the oxidation potential to 0.82 V from 1.12 V in [Co(TIM″)(C(CH_3)C_6H_4-4-^{t}Bu)Cl]PF_6 (Fig. S5, ESI†).[17] The strong influence of the axial ligand *trans* to R in the latter species supports the conclusion that the frontier molecular orbitals in the aza–cobalt–cyclopropane-bearing species differ significantly from those of the more typical Co^{III}(TIM) complexes. Additional discussion on the oxidation events can be found in the ESI.†

Conclusions

The *trans* influence of the R ligands in the Co^{III}(TIM) complexes was probed by introducing a cyano ligand as the second axial ligand. Interestingly, it was found that in the case of **1** and **3**, which bear –C(CH_2)Ph and –CH_3 ligands, respectively, the stronger σ-donating capabilities of the cyanide only minimally perturb the structural and electronic properties of the complexes. On the other hand, in **2**, which bears a 1-aza-2-cobalt-cyclopropane moiety, significant changes to the electronic nature of the Co^{III} center are observed upon substitution of the halide by cyanide, as evidenced by the changes in the absorbance spectra and cyclic voltammetry. The ability to tune the electronic structures of the metal center by altering the axial ligands suggests the possibility of using *trans* ligands to tune the photophysical/chemical properties of Co^{III}(TIM) organometallic compounds. Future efforts are also underway to probe the reactivities and catalytic capabilities of these complexes, which are inspired by the incredible scope of other vitamin B_{12} model complexes as photochemical hydrogen atom transfer catalysts[44] and photo-induced hydrogen evolution catalysts for small-molecule functionalization.[45]

Experimental

Materials

Iodomethane was purchased from Oakwood Chemicals. The dry acetonitrile used in the electrochemical studies was purchased

from Thermo Scientific. All reagents were used as received. *Trans*-[Co(TIM)Cl_2]PF_6,[40] *trans*-[Co(TIM)(C(CH_2)Ph)Cl]PF_6,[17] *trans*-[Co(TIM″)-(C(CH_3)C_6H_4-4-^{t}Bu)Cl]PF_6,[17] *trans*-[Co(TIM)$(CN)_2$]PF_6 (**4**),[22] *trans*-[Co(TIM)(CH_3)I]PF_6 (**5**),[13] and *trans*-[Co(TIM)$(CH_3)_2$]PF_6 (**6**)[14,23] were synthesized according to modified literature procedures.

Physical methods

Elemental analyses were performed by Atlantic Microlab, Inc. (Norcross, GA). UV-vis spectra were recorded on a JASCO V-780 UV-vis-NIR spectrophotometer. Fourier transform infrared (FT-IR) spectra were collected on a JASCO FT/IR-6700 spectrometer equipped with a ZnSe ATR accessory. ^{1}H NMR spectra were obtained using a Varian INOVA300 MHz or Bruker NEO300 MHz spectrometer. Electrospray ionization mass spectrometry (ESI-MS) was performed using an Advion Mass spectrometer. Cyclic voltammograms were collected on 1.0 mM solutions of the appropriate complex in dry acetonitrile at 0.1 M [^{n}Bu_4N][PF_6] electrolyte concentration using a CHI620A voltammetric analyzer, with a Pt-wire auxiliary electrode, glassy carbon working electrode (diameter = 2 mm; area = 3.14 mm^2), and Ag/AgCl pseudo-reference electrode. The working electrode was polished with alumina (0.05 μm) as needed.

Syntheses

All air-sensitive reactions were performed using standard Schlenk line techniques under dry N_2 atmosphere.

Synthesis of *trans*-[Co(TIM)(C(CH_2)Ph)(CN)]PF_6 (1). In a 100 mL flask, [Co(TIM)(C(CH_2)Ph)Cl]PF_6 (105.2 mg; 0.178 mmol) was dissolved in 50 mL of CH_3OH. A methanolic solution of KCN (20.1 mg; 0.309 mmol) was added to the red-orange solution, resulting in an immediate color change to red. After 0.5 h, the solvent was removed. The remaining residue was collected in acetone and filtered through Celite to remove insoluble K^+ salts. The addition of diethyl ether to the orange filtrate and cooling to −15 °C yielded the product as a light red-orange solid. Yield: 72.3 mg (70%). Elem. Anal. Calcd (%) for $C_{23}H_{32}N_5CoO_{0.5}PF_6$ (**1**·0.5H_2O): C, 46.8; H, 5.5; N, 11.9. Found (%): C, 46.8; H, 5.4; N, 12.2. UV-vis, λ_{max} (CH_3CN)/nm: 365 (ε/dm^3 mol^{-1} cm^{-1} 3460). IR, ν_{max}/cm^{-1} : 2130 (CN). ^{1}H NMR, δ (300 MHz; CD_3CN): 7.24–7.13 (3 H, m), 6.66–6.61 (2 H, m), 4.25 (1 H, d, J = 1.7 Hz), 3.91–3.79 (5 H, m), 3.72–3.61 (4 H, m), 2.44–2.35 (2 H, m), 2.30–2.21 (14 H, m). ESI-MS: *m*/*z* 435.8 (M^+, 100%).

Synthesis of *trans*-[Co(TIM″)(C(CH_3)C_6H_4-4-^{t}Bu)(CN)]PF_6 (2). In a 100 mL flask, [Co(TIM″)(C(CH_3)C_6H_4-4-^{t}Bu)Cl]PF_6 (100.6 mg; 0.155 mmol) was dissolved in 50 mL of CH_3OH to obtain a dark red solution. In a separate beaker, a methanolic solution of KCN (15.4 mg; 0.233 mmol) was prepared. A similar procedure and work-up described for **1** was performed to obtain compound **2** as an orange solid. Yield: 66.5 mg (87%). Elem. Anal. Calcd (%) for $C_{27}H_{43}N_5CoOPF_6$ (**2**·H_2O): C, 49.3; H, 6.6; N, 10.7. Found (%): C, 49.3; H, 6.5; N, 10.9. UV-vis, λ_{max} (CH_3CN)/nm: 420 (ε/dm^3 mol^{-1} cm^{-1} 2,530), 535sh. IR, ν_{max}/cm^{-1} : 2113 (CN). ^{1}H NMR, δ (300 MHz; CD_3CN): 7.55–6.09 (4 H, m), 4.57–4.44 (1 H, m), 4.22–3.82 (3 H, m), 3.57–3.25 (4 H, m), 3.13–2.99 (1 H, m), 2.96–2.77 (1 H, m), 2.50 (3 H, s), 2.23 (2 H, s), 2.04 (3 H, s), 1.99 (3 H, s), 1.71 (3 H, d, J = 7.3 Hz), 1.28 (12 H, d, J = 6.0 Hz). ESI-MS: *m*/*z* 493.9 (M^+, 60%), 254.6 (M^{+2}–CN + CH_3CN, 100%).

Synthesis of *trans*-[Co(TIM)(CH_3)(CN)]PF_6 (3). In a 50 mL flask, [Co(TIM)(CH_3)I]PF_6 (104.6 mg; 0.176 mmol) was dissolved in 15 mL of a 2 : 1 CH_3OH/CH_3CN mixture to yield a dark red-orange solution. KCN (13.0 mg; 0.200 mmol) was added directly to the solution, resulting in a rapid change to yellow color (~5 min). After 10 min, the solution was filtered through Celite using CH_3OH. Diethyl ether was added to the yellow-orange filtrate until the solution became cloudy. After crystallization at −15 °C for 2.5 h, a light yellow-orange solid was filtered out and washed with diethyl ether. Yield: 64.5 mg (74%). Elem. Anal. Calcd (%) for $C_{16}H_{29}N_5CoOPF_6$ (**3**·H_2O): C, 37.6; H, 5.7; N, 13.7. Found (%): C, 37.3; H, 5.8; N, 13.6. UV-vis, λ_{max} (CH_3CN)/nm: 244 (ε/dm^3 mol^{-1} cm^{-1} 28 000), 318 (3000), 402 (2880). IR, ν_{max}/cm^{-1} : 2123 (CN). ^{1}H NMR, δ_H (300 MHz; CD_3CN): 4.09–3.91 (4 H, m), 3.74–3.55 (4 H, m), 2.38 (14 H, s), 2.28–2.17 (2H, m), 0.83 (3 H, s). ESI-MS: *m*/*z* 348.4 (M^+, 100%).

X-ray crystallographic analysis

Single crystals of **1**, **2**, and **4**–**6** were obtained by slow diffusion of diethyl ether in concentrated solutions of the appropriate species in CH_3CN at −15 °C. X-ray diffraction data were obtained on a Bruker Quest diffractometer with Mo Kα radiation (λ = 0.71073 Å) at 150 K for **1**, **5**, and **6** and with Cu Kα radiation (λ = 1.54178 Å) at 150 K for **2** and **4**. Data were collected, and reflections were indexed and processed using APEX4[46] and reduced using SAINT. The space groups were assigned and the structures were solved by direct methods using XPREP within the SHELXTL suite of programs,[47] solved using ShelXT,[48] and refined using Shelxl[49,50] and Shelxle.[51] Additional details can be found in the ESI.†

Author contributions

LRS conceived the project, carried out experiments and wrote the initial draft; TR supervised the project and finished the draft.

Data availability

The data supporting this article have been included as part of the ESI.†

Conflicts of interest

There are no conflicts to declare.

Acknowledgements

This material is based upon work supported by the U.S. National Science Foundation (CHE 2350262). We thank an anonymous reviewer for spotting the I^-/Cl^- disorder in the structure of **5** and for suggesting proper refinement of the disorder.

References

1 D. C. Hodgkin, J. Kamper, M. Mackay, J. Pickworth, K. N. Trueblood and J. G. White, *Nature*, 1956, **178**, 64–66.
2 H. M. Marques, *J. Inorg. Biochem.*, 2023, **242**, 112154.
3 J. Demarteau, A. Debuigne and C. Detrembleur, *Chem. Rev.*, 2019, **119**, 6906–6955.
4 T. Wdowik and D. Gryko, *ACS Catal.*, 2022, **12**, 6517–6531.
5 A. J. Moser, B. E. Funk and J. G. West, *ChemCatChem*, 2024, **16**, e202301231.
6 A. Fihri, V. Artero, A. Pereira and M. Fontecave, *Dalton Trans.*, 2008, 5567–5569.
7 J. L. Dempsey, B. S. Brunschwig, J. R. Winkler and H. B. Gray, *Acc. Chem. Res.*, 2009, **42**, 1995–2004.
8 G. N. Schrauzer, *Acc. Chem. Res.*, 1968, **1**, 97–103.
9 P. J. Toscano and L. G. Marzilli, *Prog. Inorg. Chem.*, 1983, **31**, 105–204.
10 B. M. Alzoubi, F. Vidali, R. Puchta, C. Dücker-Benfer, A. Felluga, L. Randaccio, G. Tauzher and R. van Eldik, *Dalton Trans.*, 2009, 2392–2399.
11 W. H. Tamblyn and J. K. Kochi, *J. Inorg. Nucl. Chem.*, 1981, **43**, 1385–1389.
12 S. Hirota, S. M. Polson, J. M. Puckett, S. J. Moore, M. B. Mitchell and L. G. Marzilli, *Inorg. Chem.*, 1996, **35**, 5646–5653.
13 K. Farmery and D. H. Busch, *Inorg. Chem.*, 1972, **11**, 2901–2906.
14 K. Farmery and D. H. Busch, *J. Chem. Soc., Chem. Commun.*, 1970, 1091.
15 S. D. Banziger and T. Ren, *J. Organomet. Chem.*, 2019, **885**, 39–48.
16 T. Ren, *Chem. Commun.*, 2016, **52**, 3271–3279.
17 L. Rodriguez Segura, K. J. McGuire, A. Raghavan, J. J. Roos and T. Ren, *Organometallics*, 2024, **43**, 1057–1067.
18 T. G. Appleton, H. C. Clark and L. E. Manzer, *Coord. Chem. Rev.*, 1973, **10**, 335–422.
19 J. F. Endicott, J. Lilie, J. M. Kuszaj, B. S. Ramaswamy, W. G. Schmonsees, M. G. Simic, M. D. Glick and D. P. Rillema, *J. Am. Chem. Soc.*, 1977, **99**, 429–439.
20 H. M. Shahadat, H. A. Younus, N. Ahmad, S. Zhang, S. Zhuiykov and F. Verpoort, *Chem. Commun.*, 2020, **56**, 1968–1971.
21 C. Preston-Herrera, S. Dadashi-Silab, D. G. Oblisnky, G. D. Scholes and E. E. Stache, *J. Am. Chem. Soc.*, 2024, **146**, 8852–8857.
22 M. A. Watzky, X. Song and J. F. Endicott, *Inorg. Chim. Acta*, 1994, **226**, 109–116.
23 S. Rapsomanikis, J. J. Ciejka and J. H. Weber, *Inorg. Chim. Acta*, 1984, **89**, 179–183.
24 C. Lopez, S. Alvarez, X. Solans and M. Aguiló, *Inorg. Chim. Acta*, 1987, **133**, 101–105.
25 L. J. Cavichiolo, M. Hörner, L. D. C. Visentin and F. S. Nunes, *Anal. Sci.: X-Ray Struct. Anal. Online*, 2007, **23**, x163–x164.
26 M. Calligaris, *J. Chem. Soc., Dalton Trans.*, 1974, 1628–1631.
27 G. Tauzher, R. Dreos, A. Felluga, N. Marsich, G. Nardin and L. Randaccio, *Inorg. Chim. Acta*, 2004, **357**, 177–184.
28 L. Rodriguez Segura, S. A. Lee, B. L. Mash, A. J. Schuman and T. Ren, *Organometallics*, 2021, **40**, 3313–3322.
29 L. Randaccio, M. Furlan, S. Geremia, M. Šlouf, I. Srnova and D. Toffoli, *Inorg. Chem.*, 2000, **39**, 3403–3413.
30 S. Mebs, J. Henn, B. Dittrich, C. Paulmann and P. Luger, *J. Phys. Chem. A*, 2009, **113**, 8366–8378.
31 N. Bresciani-Pahor, L. Randaccio, E. Zangrando and P. J. Toscano, *Inorg. Chim. Acta*, 1985, **96**, 193–198.
32 A. Bigotto, E. Zangrando and L. Randaccio, *J. Chem. Soc., Dalton Trans.*, 1976, 96–104.
33 L. G. Marzilli, N. Bresciani-Pahor, L. Randaccio, E. Zangrando, R. G. Finke and S. A. Myers, *Inorg. Chim. Acta*, 1985, **107**, 139–145.
34 S. M. Polson, L. Hansen and L. G. Marzilli, *Inorg. Chem.*, 1997, **36**, 307–313.
35 K. Nakamoto, *Infrared and Raman Spectra of Inorganic and Coordination Compounds: Part A: Theory and Applications in Inorganic Chemistry*, John Wiley & Sons, Inc, 2008.
36 L. Rodriguez Segura, R. A. Clendening and T. Ren, *Organometallics*, 2023, **42**, 1717–1724.
37 I. Navizet, C. B. Perry, P. P. Govender and H. M. Marques, *J. Phys. Chem. B*, 2012, **116**, 8836–8845.
38 R. A. Firth, H. A. O. Hill, J. M. Pratt, R. G. Thorp and R. J. P. Williams, *J. Chem. Soc. A*, 1968, 2428–2433.
39 C. J. Liu, A. Thomspon and D. Dolphin, *J. Inorg. Biochem.*, 2001, **83**, 133–138.
40 S. C. Jackels, K. Farmery, E. K. Barefield, N. J. Rose and D. H. Busch, *Inorg. Chem.*, 1972, **11**, 2893–2901.
41 A. D. Torres, M. A. S. Francisco, R. R. Oliveira and A. B. Rocha, *J. Phys. Chem. A*, 2023, **127**, 3200–3209.
42 C. R. Hess, T. Weyhermüller and K. Wieghardt, *Inorg. Chem.*, 2010, **49**, 5686–5700.
43 C. R. Hess, T. Weyhermüller, E. Bill and K. Wieghardt, *Angew. Chem., Int. Ed.*, 2009, **48**, 3703–3706.
44 S. Jana, V. J. Mayerhofer and C. J. Teskey, *Angew. Chem., Int. Ed.*, 2023, **62**, e202304882.
45 K. C. Cartwright, A. M. Davies and J. A. Tunge, *Eur. J. Org. Chem.*, 2020, 1245–1258.
46 APEX4 v2022.10-1, Saint V8.40B, Bruker AXS, Inc.: Madison, WI, 2022.
47 SHELXTL suite of programs, version 6.14, 6.14; Bruker AXS Inc.: Madison, WI, 2000-2003.
48 G. M. Sheldrick, *Acta Cryst.*, 2015, **A71**, 73–78.
49 G. M. Sheldrick SHELXL2019, Göttingen, Germany, 2019.
50 G. M. Sheldrick, *Acta Crystallogr., Sect. C: Struct. Chem.*, 2015, **71**, 3–8.
51 C. B. Hübschle, G. M. Sheldrick and B. Dittrich, *J. Appl. Cryst.*, 2011, **44**, 1281–1284.